



OPEN

Contribution of glucose and glutamine to hypoxia-induced lipid synthesis decreases, while contribution of acetate increases, during 3T3-L1 differentiation

Lucie Ryskova¹, Katerina Pospisilova², Jiri Vavra³, Tomas Wolf¹, Ales Dvorak², Libor Vitek^{2,4} & Jan Polak^{1,5}✉

The molecular mechanisms linking obstructive sleep apnea syndrome (OSA) to obesity and the development of metabolic diseases are still poorly understood. The role of hypoxia (a characteristic feature of OSA) in excessive fat accumulation has been proposed. The present study investigated the possible effects of hypoxia (4% oxygen) on *de novo* lipogenesis by tracking the major carbon sources in differentiating 3T3-L1 adipocytes. Gas-permeable cultuware was employed to cultivate 3T3-L1 adipocytes in hypoxia (4%) for 7 or 14 days of differentiation. We investigated the contribution of glutamine, glucose or acetate using ¹³C or ¹⁴C labelled carbons to the newly synthesized lipid pool, changes in intracellular lipid content after inhibiting citrate- or acetate-dependent pathways and gene expression of involved key enzymes. The results demonstrate that, in differentiating adipocytes, hypoxia decreased the synthesis of lipids from glucose (44.1 ± 8.8 to 27.5 ± 3.0 pmol/mg of protein, $p < 0.01$) and partially decreased the contribution of glutamine metabolized through the reverse tricarboxylic acid cycle ($4.6\% \pm 0.2$ – $4.2\% \pm 0.1\%$, $p < 0.01$). Conversely, the contribution of acetate, a citrate- and mitochondria-independent source of carbons, increased upon hypoxia (356.5 ± 71.4 to 649.8 ± 117.5 pmol/mg of protein, $p < 0.01$). Further, inhibiting the citrate- or acetate-dependent pathways decreased the intracellular lipid content by 58% and 73%, respectively ($p < 0.01$) showing the importance of *de novo* lipogenesis in hypoxia-exposed adipocytes. Altogether, hypoxia modified the utilization of carbon sources, leading to alterations in *de novo* lipogenesis in differentiating adipocytes and increased intracellular lipid content.

Obstructive sleep apnea (OSA) is a highly prevalent disorder affecting 9–38% of the adult population¹. OSA is characterized by recurrent episodes of partial or complete collapses of the upper airway during sleep, resulting in tissue hypoxia, sleep fragmentation, and excessive daytime sleepiness. Additionally, OSA has been associated with an increased risk of developing cardiovascular and metabolic diseases, including glucose intolerance, insulin resistance, or type 2 diabetes mellitus^{2–4}, independently of other known risk factors. Although the epidemiological evidence linking OSA with metabolic impairments is convincing, the underlying molecular mechanisms remain to be elucidated.

Obesity has been identified as a main risk factor for the development of OSA^{5,6}, however, emerging evidence suggests causality in the opposite direction might also be true. For example, the severity of OSA was associated with the subsequent BMI increase⁷ as well as with limited weight loss during lifestyle intervention⁸. Suggested mechanisms linking OSA with excessive adipose tissue accumulation remain hypothetical and include cognitive and behavioral factors e.g. altered food intake and appetite regulation as well as reduced physical activity^{9–11}.

¹Department of Pathophysiology, Third Faculty of Medicine, Charles University, Ruska 87, Prague 100 00, Czech Republic. ²Institute of Medical Biochemistry and Laboratory Diagnostics, First Faculty of Medicine, Charles University, Prague, Czech Republic. ³Department of Cell Biology, Faculty of Science, Charles University, Prague, Czech Republic. ⁴Department of Internal Medicine, Institute of Medical Biochemistry and Laboratory Diagnostics, General University Hospital in Prague and First Faculty of Medicine, Charles University, Prague, Czech Republic. ⁵Department of Internal Medicine, Thomayer University Hospital, Videnska 800, Prague 140 59, Czech Republic. ✉email: jan.polak@lf3.cuni.cz

Considering the sensitivity of several adipose tissue functions to hypoxia^{12–17}, it can be hypothesized that OSA predisposes to the development of obesity through its impact on adipocyte biology, e.g. through dysregulated lipolysis, endocrine secretion, adipogenesis, differentiation and lipogenesis. In fact, previous studies have shown that hypoxic exposure promoted adipogenesis and increased intracellular lipids in adipocytes *in vitro*^{18,19}, while suppression of lipolysis was described in hypoxia-mimicking conditions²⁰. In contrast, other studies demonstrated inhibition of adipocyte differentiation^{21,22} in hypoxia and after HIF1 activation²³, demonstrating the important and sometimes opposing role of HIF1 in adipocyte differentiation, depending on the status of other signaling pathways and the stage of differentiation^{24–26}.

Hypothesis presenting OSA as a promoting factor for obesity development and maintenance is based on the fact, that mature adipose tissue is characterized by constant adipocyte turnover - a process where senescent adipocytes are replaced with newly differentiated cells from the preadipocyte pool²⁷. It has been determined that average adipocyte survival, independent of age or degree of obesity, is approximately 10 years²⁸. Hypoxia, as a hallmark of OSA, could thus impact precursors as well as differentiating cells (on their trajectory from preadipocytes to adipocytes) and modify them towards obesity phenotype, however, timing and consequences of such hypoxic stimulus as well as magnitude of the effect on lipid accumulation remain unknown. Similarly, hypoxia was shown to increase lipid accumulation in adipocytes, however, sources of excessive intracellular lipids remain unclear with the possible contribution of *de novo* lipogenesis as well as transport of fatty acids from the extracellular compartment. As previous studies reported reduced, rather than increased, fatty acids transport into adipocytes and muscle cells under hypoxic conditions^{29,30}, probably due to decreased expression of FATP1 and CD36 transporters, intracellular lipid synthesis becomes a plausible source for elevated intracellular lipids. Intracellular acetyl-CoA pool, representing the source metabolite for *de novo* lipogenesis, is maintained by the metabolism of glucose (and other glycolytic metabolites) and branched-chain amino acids in tricarboxylic acid cycle (Krebs cycle) generating citrate which is subsequently exported out of the mitochondria and converted to acetyl-Co and oxaloacetate³¹. Furthermore, glutamine was identified as an important source of citrate and acetyl-CoA, particularly under hypoxic conditions through reverse tricarboxylic acid cycle (rTCA)^{32–35}. Finally, acetate, circulating in plasma in micromolar concentrations, represents an important source of acetyl-CoA in mammalian cells^{36–40}, although, its role in hypoxia-induced lipogenesis in adipocytes remains unknown.

The present study aimed to investigate whether exposure to hypoxia during differentiation of preadipocytes into adipocytes would affect intracellular lipid content and whether the effect of hypoxic exposure is dependent on the stage of differentiation (early versus late adipocytes). Furthermore, the study investigated hypoxia-induced changes in sources for *de novo* lipogenesis during adipocyte differentiation. To achieve this goal, we employed 3T3-L1 cells and exposed them to hypoxic or control conditions using a gas-permeable cultureware^{22,41–43}. Subsequently, the gene expression change of key enzymes and the incorporation of carbon molecules originating from isotope-labeled glucose (¹⁴C-glucose), acetate (¹⁴C-acetate) or glutamine (¹³C-glutamine) was traced into lipids to assess *de novo* lipogenesis in adipocytes after 7 days (early adipocytes) or 14 days (late adipocytes) of differentiation. The contribution of citrate- or acetate-dependent pathways to the lipid pool during adipocyte differentiation under hypoxia was investigated using ATP-dependent citrate lyase inhibitor (SB 204990) or Acetyl-CoA synthetase 2 inhibitor (ACSS2i). The outcomes of this study provide molecular evidence supporting the hypothesis that OSA (hypoxia) causally contributes to the development and/or maintenance of obesity at the cellular level via changes in *de novo* lipogenesis.

Results

rTCA contribution to *de novo* lipogenesis

The exposure to hypoxia did not affect palmitate accumulation in early adipocytes (Fig. 1A). However, prolonged cultivation under hypoxic exposure significantly increased intracellular palmitate accumulation in late adipocytes from $13.4\% \pm 2.1$ – $31.4\% \pm 6\%$ ($p < 0.01$) compared to control conditions and from $6.3\% \pm 1$ – $31.4\% \pm 6\%$ ($p < 0.01$) compared to hypoxia-exposed early adipocytes. Stably labeled glutamine was used to investigate whether hypoxic conditions activated rTCA during adipocyte maturation, thus contributing to an increased lipid pool. Glutamine labeled at position C₅ was used to trace the direct contribution of rTCA to *de novo* lipogenesis. The results showed that exposure to hypoxia increased ¹³C incorporation in early adipocytes from $3.2\% \pm 0.2$ – $4.6\% \pm 0.2\%$ vs. control conditions ($p < 0.01$) and from $3.0\% \pm 0.3$ – $4.0\% \pm 0.1\%$ vs. control conditions ($p < 0.01$) in late adipocytes (Fig. 1B). Furthermore, ¹³C incorporation decreased in hypoxia-exposed late adipocytes compared to hypoxia-exposed early adipocytes from $4.6\% \pm 0.2$ – $4.0\% \pm 0.1\%$ ($p < 0.01$). In parallel support to these findings, analysis of rTCA-related metabolite labeling was conducted using glutamine containing ¹³C at the C₁ position. The results showed that ¹³C incorporation to citrate (Fig. 1C) after exposure to hypoxia increased in early adipocytes from 3.4 to 3.7% ($p < 0.01$) compared to control conditions and decreased in late adipocytes from 3.2 to 2.9% ($p < 0.02$) compared to control conditions. Similarly, hypoxia increased ¹³C incorporation to malate (Fig. 1D) in early adipocytes from 5.5 to 6.0% vs. control conditions ($p < 0.01$) but showed no effect in late adipocytes.

Glucose and acetate contribution to *de novo* lipogenesis

The ¹⁴C incorporation studies were performed to investigate hypoxia-induced changes in pathways of *de novo* lipogenesis during adipocyte maturation. To evaluate the contribution of glucose to a newly synthesized lipid pool, ¹⁴C-glucose was employed. Hypoxia significantly increased ¹⁴C-glucose incorporation in early adipocytes from 14.2 ± 3.3 pmol/mg of protein to 44.1 ± 8.8 pmol/mg of protein ($p < 0.01$) compared to control conditions (Fig. 2A). In hypoxia-exposed late adipocytes, ¹⁴C-glucose incorporation dropped from 44.1 ± 8.8 pmol/mg of protein to 27.5 ± 3.0 pmol/mg of protein ($p < 0.01$) compared to hypoxia-exposed early adipocytes and was sustained at control level. Further, the contribution of acetate, an important carbon source for *de novo* lipogenesis, was investigated by tracing ¹⁴C-acetate in the lipid pool. The results showed that hypoxia exposure

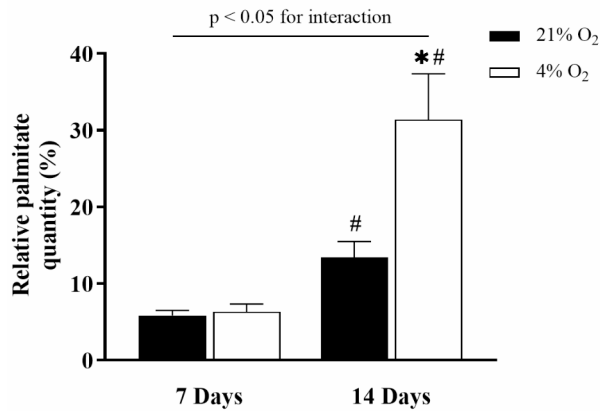
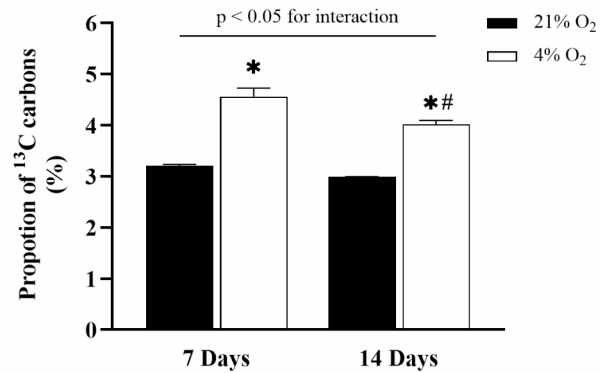
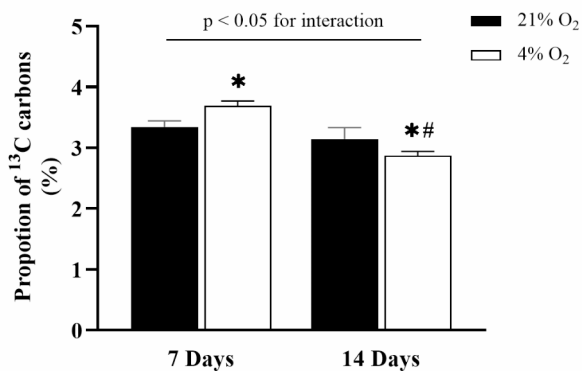
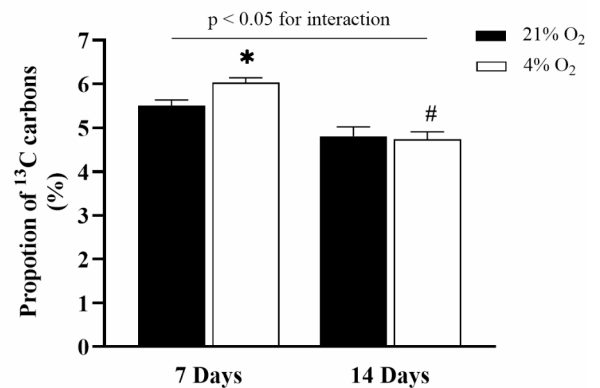
A. Total palmitate**B. ¹³C-glutamine incorporation to lipids****C. ¹³C-citrate incorporation to lipids****D. ¹³C-malate incorporation to lipids**

Fig. 1. The effect of hypoxia on lipid quantity and rTCA contribution to *de novo* lipogenesis during adipocyte differentiation. The effect of hypoxia on intracellular palmitate content in early and late adipocytes (A). Percentage of ¹³C derived via rTCA from ¹³C₅-labeled glutamine into intracellular palmitate (B). Percentage of ¹³C derived from ¹³C₁-labeled glutamine into citrate (C) and malate (D), representing the rTCA-generated metabolites. Data are presented as the mean ± SD, N=9. Two-way ANOVA was performed followed by Tukey's post-hoc test. **p* < 0.05 for comparison 4% O₂ vs. 21% O₂; #*p* < 0.05 for comparison 7 Days vs. 14 Days.

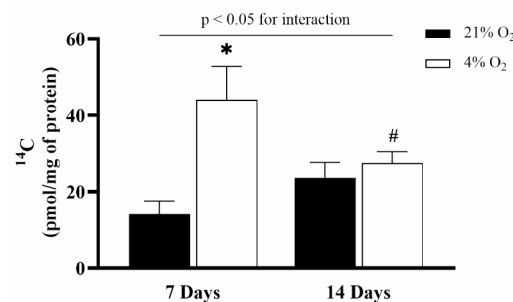
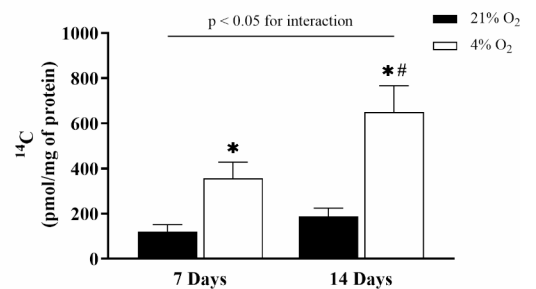
A. ¹⁴C-glucose incorporation to lipids**B. ¹⁴C-acetate incorporation to lipids**

Fig. 2. The effect of hypoxia on glucose and acetate contribution to *de novo* lipogenesis during adipocyte differentiation. Incorporation study of ¹⁴C radiolabeled isotopes assessing glucose (A) or acetate (B) contribution to the intracellular lipid pool in early and late adipocytes. Data are presented as the mean ± SD, N=9. Two-way ANOVA was performed followed by Tukey's post-hoc test. **p* < 0.05 for comparison 21% O₂ vs. 4% O₂; #*p* < 0.05 for comparison 7 Days vs. 14 Days.

increased ^{14}C -acetate incorporation in early adipocytes from 119.5 ± 31.9 pmol/mg of protein to 356.5 ± 71.4 pmol/mg of protein ($p < 0.01$) compared to control conditions. Moreover, incorporation increased significantly from 187.0 ± 37.5 pmol/mg of protein to 649.8 ± 117.5 pmol/mg of protein ($p < 0.01$) in hypoxia-exposed late adipocytes compared to control conditions and by 82% ($p < 0.01$) compared to hypoxia-exposed early adipocytes (Fig. 2B).

Gene expression analysis during differentiation under hypoxia

The analysis of gene expression during differentiation under hypoxia focused on key enzymes involved in glucose, glutamine, and acetate metabolic pathways. The relative expression of the *PDHA1* gene showed a significant interaction between experimental groups ($p = 0.01$) (Fig. 3A). Specifically, the expression significantly decreased in normoxic late adipocytes, from 22.5 ± 2.9 to 13.9 ± 4.1 $2^{-\Delta\text{CT}}$ ($p = 0.02$) when compared to normoxic early adipocytes, and showed a slight (non-significant) decrease in hypoxic late adipocytes to 18.3 ± 5.1 $2^{-\Delta\text{CT}}$ ($p = 0.06$). Hypoxia exposure did not significantly affect *IDH1* or *IDH2* gene expression (Fig. 3B and C). However, hypoxia led to a significant increase in *ACLY* gene expression in late adipocytes, rising to 14.7 ± 4.4 $2^{-\Delta\text{CT}}$ compared to 6.5 ± 2.6 $2^{-\Delta\text{CT}}$ in normoxic early adipocytes ($p = 0.01$), and compared to 8.4 ± 1.8 $2^{-\Delta\text{CT}}$ in hypoxic early adipocytes ($p = 0.02$) (Fig. 3D). No significant increase was observed when comparing hypoxic late adipocytes to normoxic late adipocytes (10.0 ± 2.8 $2^{-\Delta\text{CT}}$). Similarly, hypoxia-exposed late adipocytes exhibited a significant increase in *ACSS2* gene expression, reaching 4.8 ± 2.2 $2^{-\Delta\text{CT}}$ compared to 1.0 ± 0.4 $2^{-\Delta\text{CT}}$ in normoxic early adipocytes ($p = 0.01$), and 1.7 ± 0.8 $2^{-\Delta\text{CT}}$ in hypoxic early adipocytes ($p = 0.02$). However, there was no significant difference compared to control late adipocytes, as summarized in Fig. 3E.

Determination of total lipid content

Inhibition experiments targeting citrate- and acetate-dependent pathways were performed to support the findings from the incorporation studies described above. The results confirmed that prolonged hypoxia significantly increased the total lipid content during differentiation, rising from 112.3 ± 23.0 $\mu\text{g}/\text{mg}$ of protein to 196.2 ± 45.7 $\mu\text{g}/\text{mg}$ of protein ($p < 0.01$) in comparison to late normoxic adipocytes, and from 19.4 ± 3.1 $\mu\text{g}/\text{mg}$ of protein ($p < 0.01$) when compared to early hypoxic adipocytes (Fig. 4A). Furthermore, the inhibition of ATP-citrate lyase (*ACLY*) had no impact on early adipocytes. However, a reduction in total lipid content, from 196.2 ± 45.7 $\mu\text{g}/\text{mg}$ of protein to 82.7 ± 8.9 $\mu\text{g}/\text{mg}$ of protein ($p = 0.01$), was observed during differentiation. Notably, hypoxia exposure in inhibitor-treated cells did not show any effect during the differentiation period. Similarly, inhibition of acetate-dependent acetyl-CoA synthetase 2 (*ACSS2*) did not affect lipid content in early adipocytes (Fig. 4B), yet in differentiated late adipocytes, *ACSS2* inhibition led to a dramatic 73% reduction in lipid content, from 196.2 ± 45.7 $\mu\text{g}/\text{mg}$ of protein to 52.3 ± 7.0 $\mu\text{g}/\text{mg}$ of protein ($p < 0.01$). However, hypoxia exposure did not significantly affect the *ACSS2* inhibitor-treated cells.

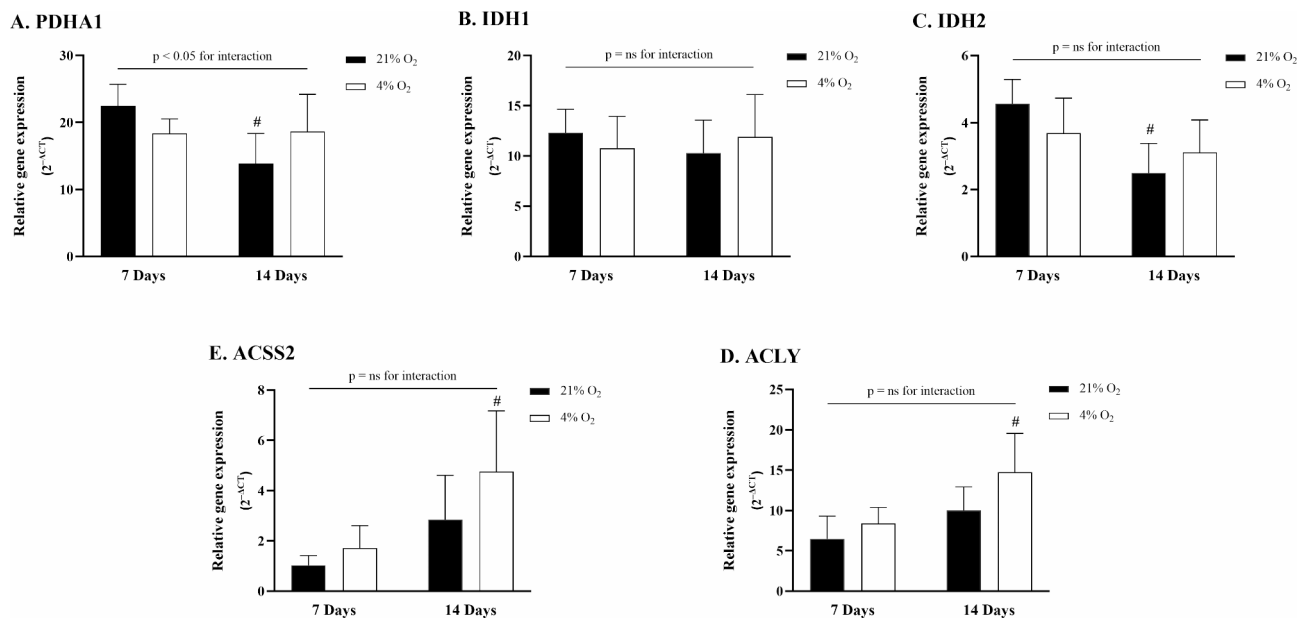


Fig. 3. Gene expression change of selected enzymes during adipocytes differentiation under hypoxia. Quantitative real-time PCR was employed to assess gene expression of (A) pyruvate dehydrogenase E1 alpha 1 (*PDHA1*), (B) ATP citrate lyase (*ACLY*), and (C) acyl-CoA synthetase short-chain family member 2 (*ACSS2*), (D) isocitrate dehydrogenase 1 (*IDH1*), (E) isocitrate dehydrogenase 2 (*IDH2*). All values are expressed as $2^{-\Delta\text{CT}}$. Data are presented as the mean \pm SD, $N = 6$. Two-way ANOVA test was performed followed by Tukey's post-hoc test. * $p < 0.05$ for comparison 4% O₂ vs. 21% O₂; # $p < 0.05$ for comparison 7 Days vs. 14 Days; ns = non-significant.

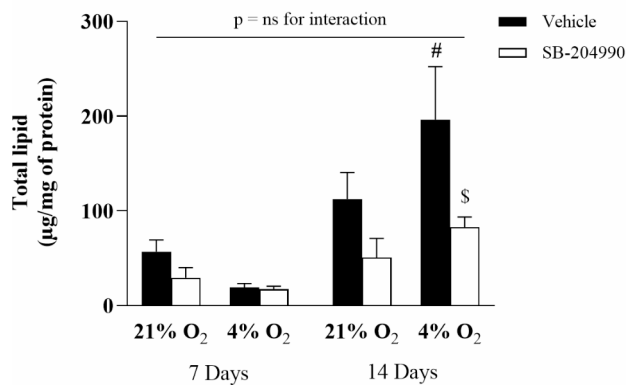
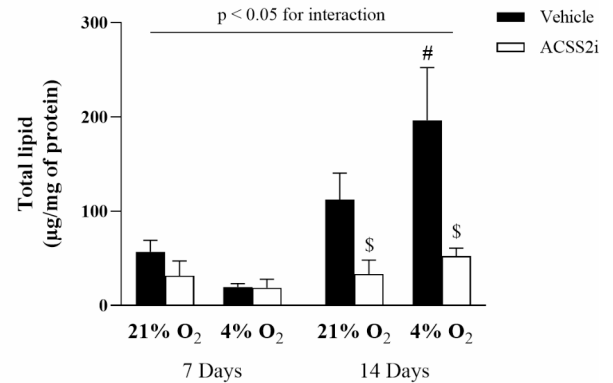
A. ACLY inhibitor SB-204990**B. Ac-CoA synthase inhibitor1**

Fig. 4. The effect of hypoxia on total lipid content after inhibition of citrate- or acetate-dependent pathways. Intracellular lipid accumulation in 3T3-L1 adipocytes after 7 or 14 days exposed to hypoxia (A) ATP-citrate lyase inhibitor (SB-204990), (B) acetate-dependent acetyl-CoA synthetase 2 inhibitor (Ac-CoA synthase inhibitor1). Data are presented as the mean \pm SD, $N=3$. A three-way ANOVA test was performed followed by Tukey's post-hoc test. * $p < 0.05$ for comparison 4% O₂ vs. 21% O₂; # $p < 0.05$ for comparison 7 Days vs. 14 Days; \$ $p < 0.05$ for comparison treatment vs. vehicle; ns = non-significant.

Discussion

This study aimed to investigate whether OSA causally contributes to the development of obesity through changes in the regulation of adipocyte lipogenesis during differentiation. Exposure to hypoxia during differentiation increased the intracellular lipid content in adipocytes. Furthermore, hypoxia-induced lipogenesis from glucose and glutamine (provided through the rTCA cycle) decreased, while lipogenesis from acetate increased during adipocyte differentiation.

Obesity represents a major risk factor in OSA development⁶. The reverse relationship has been also suggested, that is, OSA can promote obesity, for example, via increased energy intake, reduced energy expenditure, modified food preferences, and altered lifestyle⁴⁴. An additional mechanism linking OSA with obesity development was explored in this paper; specifically, hypoxia-induced molecular adaptations in adipocytes during their differentiation from preadipocytes. We speculated that adipose tissue hypoxia associated with severe OSA⁴⁵ affects adipocyte functions, including lipid synthesis during adipocyte maturation. In fact, previous studies have shown that hypoxia increases the levels of adipogenic markers and total lipid content in adipocytes^{18,46}, suggesting accelerated adipocyte differentiation. However, the contribution of various substrates utilized for newly synthesized lipids under hypoxic exposure remained unclear. Additionally, constant adipocyte turnover (death) induces the replenishment of mature adipocytes from precursor cells²⁷. Immature preadipocytes are thus exposed to hypoxia with unknown consequences. The present study showed that hypoxic exposure during adipocyte maturation not only promotes lipogenesis but also shifts the sources of acetyl-CoA used for lipid synthesis from glucose (and, to a minor extent, glutamine) to acetate.

De novo lipid synthesis serves two major functions in the cellular context. First, newly produced lipids are used for a variety of purposes within the cell, such as for the construction of biological membranes, trafficking vesicles, signaling molecules, or energy storage⁴⁷, which is a major physiological function of adipocytes. Lipid synthesis also represents a conserved adaptive mechanism to help cells (particularly mitochondria) survive under hypoxic conditions⁴⁸. Limited oxygen availability results in the lagging transport of protons and electrons through the mitochondrial respiratory chain, with subsequent elevation of the NADH/NAD⁺ ratio in mitochondria⁴⁹. *De novo* lipogenesis serves as a salvage mechanism for depositing hydrogen ions after transporting them out of mitochondria through the activity of the NAD(P)⁺ transhydrogenase enzyme in the form of NADPH⁵⁰, which is subsequently combined with acetyl-CoA in the process of lipogenesis. Under normoxic conditions, pyruvate derived from glycolysis represents a primary source of acetyl-CoA—a building block for intracellular *de novo* lipid synthesis⁵¹. Even though glucose uptake is enhanced in adipocytes as a response to hypoxic exposure¹², the metabolic fate of glucose differs between early and late adipocytes. As early adipocytes are characterized by lower energy demands⁵², hypoxic exposure results in glucose being partially utilized for ATP production through anaerobic glycolysis. However, a substantial part of glucose is also metabolized to pyruvate, transported to mitochondria, and subsequently converted to acetyl-CoA for use in *de novo* lipogenesis. In fact, the present study showed that hypoxia promoted incorporation of glucose-derived carbons to lipids by 210% in early adipocytes. In contrast, mature adipocytes, with higher energy demands⁵², were not capable of utilizing glucose for lipid synthesis under hypoxia, probably because of increased demand for anaerobic ATP production; hence, the majority of glucose is diverted to lactate rather than acetyl-CoA. These observations correlate with the decreased *PDHAI* gene expression, which codes the enzyme important for the conversion of pyruvate to acetyl-CoA. Alternative carbon (acetyl-CoA) sources are thus needed to secure adipocyte homeostasis in hypoxic conditions.

Cells are endowed with a powerful mechanism, referred to as rTCA or “reverse Krebs cycle,” that secures the replenishment of the acetyl-CoA pool from sources other than glucose. Specifically, the conversion of glutamine to α -ketoglutarate and subsequent reductive carboxylation to citrate provides sufficient quantities of acetyl-CoA for biosynthetic needs. Reverse TCA has been identified as a major source of acetyl-CoA under hypoxic conditions, especially in the context of cancer cells where 60–80% of acetyl-CoA is derived through this pathway⁵³. The results of the present study demonstrate that identical responses are employed also in adipocytes, particularly in immature cells, where incorporation of ¹³C from glutamine to palmitate increased by 42% under hypoxia together with appropriate enrichment of precursor metabolites (citrate and malate). With continued hypoxic exposure during adipocyte differentiation, the contribution of rTCA decreased, as demonstrated by the reduced ¹³C enrichment of citrate and malate from labeled glutamine and by the decreasing proportion of ¹³C carbons in lipids. Additionally, gene expression analysis of two genes *IDH1* and *IDH2*, key enzymes for the reductive pathway, showed no significant changes under hypoxia exposure. Altogether, these results suggest the employment of yet another source of carbon for *de novo* lipogenesis - the often-neglected acetate.

Acetate from intracellular processes or extracellular sources can reach plasma concentrations of 50–650 μ M in humans and rodents⁴⁰ and has been identified as a significant source of acetyl-CoA and lipogenesis independently of glucose transport or citrate or mitochondrial metabolism⁵⁴. Unlike other carbon donors for *de novo* lipogenesis, acetate freely diffuses through cellular membranes and is converted to acetyl-CoA in a one-step reaction. The findings of the present study indicate that the acetate-dependent pathway plays a significant role in lipogenesis in differentiated adipocytes, as inhibition of ACSS2 resulted in a 15% greater reduction in total lipid content compared to ACLY inhibition, implying that ACLY was less capable of compensating for the loss of ACSS2 function in these cells. Furthermore, various cancer cells increased the production of acetyl-CoA from acetate by over 50% in hypoxic conditions^{39,55}. The present study showed that acetate is the only lipogenic carbon source in adipocytes with increased contribution during adipocyte differentiation under hypoxic conditions. This observation is in line with studies reporting that hypoxia decreases glucose and increases acetate utilization for fatty acid biosynthesis in hypoxic/cancer cells^{40,55}. Further studies are warranted, however, based on the observations presented in this study. It can be hypothesized that adipocyte differentiation under hypoxic conditions (e.g. OSA) promotes *de novo* lipogenesis from acetate. Notably, in adipose tissue, the incorporation rate of acetate into total lipids was measured as ~40% higher than that of glucose⁵⁶. Future studies will need to elucidate whether such modulation is clinically relevant in the context of obesity development in patients with OSA.

Several limitations of the experimental procedures used in this study need to be considered. First, a cell culture model of OSA was employed^{41,57–59} that enabled the investigation of direct effects of hypoxia on adipocytes. However, the responses induced by OSA in people are rather more complex, involving hypoxia and sleep fragmentation as well as stress and neuroendocrine and cognitive interactions. Second, as differentiating adipocytes synthesize lipids primarily *de novo*⁶⁰, the present study investigated the impact of hypoxia and differentiation on this pathway; however, another important source of intracellular lipids—fatty acid uptake together with regulation of lipolysis and whole-cell lipid turnover needs to be combined to obtain a comprehensive picture of adipocyte life in hypoxic conditions. Third, the level of 4% O₂ was used to induce hypoxia, as it represents the equivalent to oxygen concentration expected in the adipose tissues of patients with OSA and measured in rodent OSA models⁴⁵. Finally, it should be noted that the contribution of rTCA pathway to total adipocyte lipid content is rather limited, as the ¹³C enrichment of palmitate represented only 5% of total intracellular palmitate carbons. To clarify these results, the ¹³C-glutamine labeled at the C5 position was used to directly trace the lipid enrichment specifically through reductive metabolism, given the stoichiometry of citrate. Similarly, the ¹³C labelled carbon can be tracked in TCA metabolites only through reductive metabolism, as in the oxidative pathway they are lost as ¹³CO₂ in the reaction catalyzed by 2-KG dehydrogenase³⁴. In conclusion, the present study showed that exposure of differentiating adipocytes to hypoxia increased intracellular palmitate content. Adipocytes differentiated under hypoxic conditions exhibited augmented *de novo* lipogenesis from acetate, while the contribution of glucose and rTCA to the synthesized lipids diminished.

Materials and methods

Cell culture maintenance and hypoxia induction

Murine 3T3-L1 preadipocytes (Zenbio, Inc., USA), at an initial density of 4000 cells/cm², were cultured in 24-well fluorocarbon-bottom plates (94.6000.014; Sarstedt AG & Co, Germany) for ¹⁴C incorporation studies or in 50 mm fluorocarbon-bottom dishes (94.6077.410; Sarstedt AG & Co) for ¹³C incorporation studies, gene expression analysis and lipogenesis determination. The cells were cultured in complete medium containing high glucose DMEM (D6429; Merck, USA), 10% FBS (F6178; Merck), 1% penicillin–streptomycin (P4333; Merck), and 1% HEPES (H0887; Merck) at 37 °C and 5% CO₂. At 2 days postconfluency (day 0), the cells were induced to differentiate into mature adipocytes for 2 days using complete medium supplemented with 0.5 mM 3-Isobutyl-1-methylxanthine (I5879; Merck), 0.25 μ M dexamethasone (D2915; Merck), 1 μ g/ml insulin (I9278; Merck), and 2 μ M rosiglitazone (71740; Cayman Chemical Com., USA)⁶¹. After 2 days, the cells were cultured in complete medium containing 1 μ g/ml insulin for further days up to their fully differentiated state (day 14). To induce hypoxia, on day 0, the cells were placed in modular incubators (Billups-Rothenberg Inc., USA) that were inflated with a mixture of 4% O₂ + 5% CO₂ (Linde Gas a.s., Czech Republic). The control groups were maintained in 21% O₂ + 5% CO₂. The cells were processed for experiments on day 7 (the starting point of the lipid accumulating phase in 3T3-L1 cells) and on day 14 of the differentiation, when the lipids represent 80% of total cell mass and cells are considered as fully matured^{17,61,62}. *Analysis of rTCA activation.*

To assess the activation of rTCA under hypoxic conditions, stable labeled ¹³C-1]-glutamine (CLM-3612-PK; Cambridge Isotope Laboratories, Inc., USA) or unlabeled glutamine (for control experiments) were employed. The cells were cultured in complete medium containing 2.5 mM ¹³C-1]-glutamine or unlabeled glutamine for

24 h and then immediately frozen on dry ice blocks. The cells were washed with cold PBS and lysed in chloroform/methanol/water (2:1:1). The suspension was vortexed and centrifuged for 1000 g/10 min. The separated polar phase was collected and subsequently lyophilized overnight. Derivatization of dry samples was proceeded at 65 °C for 75 min using chlorotrimethylsilane/*N*, *O*-Bis (trimethylsilyl) acetamide/pyridine (1/2/4 v/v/v) and the samples were further analyzed via gas chromatography coupled with mass spectrometry (GC/MS) on an Agilent 6890 coupled to an Agilent 5973 mass spectrometer and Agilent ChemStation software (Agilent Technologies, Palo Alto, CA) as described previously^{43,63}. The ratio ¹³C to ¹²C of rTCA-related metabolites (m/z settings: citrate 274/273; malate 336/335) was calculated. Non-labeled control samples were used as natural ¹³C background. The results were expressed as the percentage of ¹³C incorporation to the total carbon amount of each metabolite.

Contribution of rTCA to de novo lipid synthesis

The cells were cultured in a complete medium containing 2.5 mM ¹³C-5]-glutamine (CLM-1822-H-PK; Cambridge Isotope Laboratories, Inc.) or unlabeled glutamine (as a control) throughout the whole differentiation period (7 or 14 days). The cells were then washed with cold PBS, lysed in chloroform/methanol/water (2:1:1), vortexed, and centrifuged for 1000 g/10 min to separate the fractions. The extracted nonpolar phase was dried using nitrogen gas, and lipid hydrolysis proceeded via incubation in 80% ethanol with 0.5 mM KOH (60 °C, 20 min). The suspension was neutralized with acetic acid, the lipids were extracted to hexane added 1/1 v/v and, after drying using nitrogen gas, derivatized with diazomethane for 20 min. Diazomethane solution was briefly evaporated and re-dissolved samples in 200 µL of hexane were analyzed via GC/MS using a mobile phase (1 ml/min) in a RESTEK Rxi-5ms (15 m × 0.25 mm, ID: 0.25 µm) column. The oven program started with 1 min 100° C hold, then increased at 10 °C/min to 250 °C followed by 20 °C/min to 310 °C. The single MS operated in selective ion monitoring mode with m/z settings: 270, 271, 272, 273, 274 and 275⁴³. Palmitate was analyzed as a representative fatty acid. Data were calculated as the percentage of ¹³C incorporation to the total carbon amount of palmitate. A total ¹²C palmitate content (m/z settings: 270) was analyzed to internal standard (m/z settings: 284) and normalized to protein content.

¹⁴C-glucose and ¹⁴C-acetate incorporation

3T3-L1 differentiated adipocytes were incubated in a serum-free medium 24 h before incorporation. On the day of the experiment, the medium was removed, and the cells were washed twice with glucose-free Krebs Ringer buffer (KRB; 130 mM NaCl, 10 mM MgSO₄, 2.5 mM NaH₂PO₄, 4.6 mM KCl, 2.5 mM CaCl₂, 2.5 mM sodium pyruvate, and 5 mM HEPES, pH 7.4, 37 °C). For glucose or acetate incorporation study, 2 µM D-¹⁴C(U)-glucose (NEC042 × 050UC; Perkin Elmer, USA) or 2 µM [1,2-¹⁴C]-acetate (NEC553050UC; Perkin Elmer) were added into KRB and incubated for 120 min at 37 °C in normoxic (control) or hypoxic conditions. After incubation, the cells were placed immediately on ice and the incubation solution was discarded. The cells were washed thrice with cold KRB and subsequently lysed for 2 h at 4 °C using 0.15 M NaOH^{64–66}. The lysates were collected and neutralized with 1 M HCl and subjected to total lipid extraction using the Bligh-Dyer extraction method⁶⁷. The radioactivity of the sample mixture with UltimaGold LSC cocktail (Perkin Elmer) was measured using a PerkinElmer TriCarb 2900-TR liquid scintillation counter (pre-measuring = 1 min, measuring = 5 min) and the effect of naturally occurring ¹⁴C was corrected. The data were normalized to protein content⁶⁸.

Gene expression analysis

Total RNA was isolated using High Pure RNA Isolation Kit (11828665001, Roche Diagnostics, Switzerland) and transcribed to cDNA with High-Capacity cDNA Reverse Transcription Kit (4368814, Roche Diagnostics) according to the manufacturer's instructions. Quantitative RT-PCR reactions were performed using the TaqMan probes (4331182, Applied Biosystems, USA) of Pdha1 (Mm00468675_m1), Acly (Mm01302282_m1), Accs2 (Mm00480101_m1), Idh1 (Mm00516030_m1), Idh2 (Mm00612429_m1), Gusb (Mm01197698_m1), Tbp (Mm01277042_m1) and Real Time PCR cyler ABI 750 (ThermoFisher Scientific, USA). TBP (Mm01277042_m1) and GUSB (Mm01197698_m1) were used as endogenous controls. Data were presented as the relative gene expression change using the 2^{-ΔCT} method.

Determination of lipogenesis

To assess the contribution (activity) of citrate- or acetate-dependent pathways to the intracellular lipid pool we exposed the cells to hypoxia with selected specific inhibitors for 7 or 14 days. Cells were treated with 40 µM SB-204,990 (HY-15245; MedChemExpress, USA) to inhibit the ATP-dependent citrate lyase⁴³ or with 20 µM ACSS2i (HY-104032; MedChemExpress, USA) to inhibit the acetate-dependent acetyl-CoA synthetase²⁷⁰. Both drugs were dissolved in DMSO, while the identical volume of DMSO was used in culture media as the control group. After the cultivation period, the cells were placed immediately on ice and the media was discarded. The cells were washed twice with cold PBS. Intracellular lipids were extracted using the Bligh-Dyer extraction method and quantified using a neutral lipids assay kit (ab242307, Abcam, UK) according to the manufacturer's protocol. Lipid content was normalized to the total protein amount for each experimental group.

Statistical analysis

Statistically significant differences between groups (7 days 21% O₂, 7 days 4% O₂, 14 days 21% O₂, and 14 days 4% O₂) were analyzed using two-way analysis of variance (ANOVA) followed by Tukey's post-hoc tests. Three-way ANOVA (F1 × F2 × F3; hypoxia × time × drug treatment), followed by Tukey's post-hoc test, was performed for experiments with inhibitors. GraphPad Prism 10 (GraphPad Software Inc, USA) was used for figure production and statistical analyses. The value of *p* ≤ 0.05 was considered statistically significant. Data are presented as the mean ± SD of nine (incorporation studies), six (qPCR) or three replicates (inhibitors studies).

Data availability

The data presented in this study are available on request from the corresponding author.

Received: 7 September 2023; Accepted: 8 November 2024

Published online: 15 November 2024

References

1. Senaratna, C. V. et al. Prevalence of obstructive sleep apnea in the general population: A systematic review. *Sleep. Med. Rev.* **34**, 70–81 (2017).
2. Briançon-Marjollet, A. et al. The impact of sleep disorders on glucose metabolism: Endocrine and molecular mechanisms. *Diabetol. Metab. Syndr.* **7**, 25 (2015).
3. Kent, B. D., McNicholas, W. T. & Ryan, S. Insulin resistance, glucose intolerance and diabetes mellitus in obstructive sleep apnoea. *J. Thorac. Dis.* **7**, 1343–1357 (2015).
4. Aurora, R. N. & Punjabi, N. M. Obstructive sleep apnoea and type 2 diabetes mellitus: A bidirectional association. *Lancet Respir. Med.* **1**, 329–338 (2013).
5. Gottlieb, D. J. & Punjabi, N. M. Diagnosis and management of obstructive sleep apnea: A review. *JAMA.* **323**, 1389–1400 (2020).
6. Jehan, S. et al. Obstructive sleep apnea and obesity: Implications for Public Health. *Sleep. Med. Disord.* **1**, (2017).
7. Brown, M. A. et al. The impact of sleep-disordered breathing on body Mass Index (BMI): The Sleep Heart Health Study (SHHS). *Southwest. J. Pulm Crit. Care.* **3**, 159 (2011).
8. Borel, A. L. et al. Sleep apnoea attenuates the effects of a lifestyle intervention programme in men with visceral obesity. *Thorax.* **67**, 735–741 (2012).
9. Zuraikat, F. M. et al. Dimensions of sleep quality are related to objectively measured eating behaviors among children at high familial risk for obesity. *Obes. (Silver Spring).* **31**, 1216–1226 (2023).
10. Shechter, A. Obstructive sleep apnea and energy balance regulation: A systematic review. *Sleep. Med. Rev.* **34**, 59–69 (2017).
11. Shechter, A. Effects of continuous positive airway pressure on energy balance regulation: A systematic review. *Eur. Respir. J.* **48**, 1640–1657 (2016).
12. Trayhurn, P. Hypoxia and adipose tissue function and dysfunction in obesity. *Physiol. Rev.* **93**, 1–21 (2013).
13. Yin, J. et al. Role of hypoxia in obesity-induced disorders of glucose and lipid metabolism in adipose tissue. *Am. J. Physiol. Endocrinol. Metab.* **296**, 333–342 (2009).
14. Uchiyama, T., Ota, H., Ohbayashi, C. & Takasawa, S. Effects of intermittent hypoxia on Cytokine expression involved in insulin resistance. *Int. J. Mol. Sci.* **22**, (2021).
15. Lempesis, I. G., van Meijel, R. L. J., Manolopoulos, K. N. & Goossens, G. H. Oxygenation of adipose tissue: A human perspective. *Acta Physiol. (Oxf)* **228**, (2020).
16. Ota, H. et al. Relationship between intermittent hypoxia and type 2 diabetes in Sleep Apnea Syndrome. *Int. J. Mol. Sci.* **2019**, **20**, 4756 (2019).
17. Oates, E. H. & Antoniewicz, M. R. 13 C-Metabolic flux analysis of 3T3-L1 adipocytes illuminates its core metabolism under hypoxia. *Metab. Eng.* **76**, 158–166 (2023).
18. Weissenstein, M. et al. Adipogenesis, lipogenesis and lipolysis is stimulated by mild but not severe hypoxia in 3T3-L1 cells. *Biochem. Biophys. Res. Commun.* **478**, 727–732 (2016).
19. Suzuki, T., Shinjo, S., Arai, T., Kanai, M. & Goda, N. Hypoxia and fatty liver. *World J. Gastroenterol.* **20**, 15087–15097 (2014).
20. Michailidou, Z. et al. Adipocyte pseudohypoxia suppresses lipolysis and facilitates benign adipose tissue expansion. *Diabetes.* **64**, 733–745 (2015).
21. Kim, K. H., Song, M. J., Chung, J., Park, H. & Kim, J. B. Hypoxia inhibits adipocyte differentiation in a HDAC-independent manner. *Biochem. Biophys. Res. Commun.* **333**, 1178–1184 (2005).
22. Musutova, M., Weissenstein, M., Koc, M. & Polak, J. Intermittent Hypoxia stimulates Lipolysis, but inhibits differentiation and De Novo Lipogenesis in 3T3-L1 cells. *Metab. Syndr. Relat. Disord.* **18**, 146–153 (2020).
23. Shao, M. et al. Pathologic HIF1 α signaling drives adipose progenitor dysfunction in obesity. *Cell. Stem Cell.* **28**, 685–701e7 (2021).
24. Floyd, Z. E., Kilroy, G., Wu, X. & Gimble, J. M. Effects of prolyl hydroxylase inhibitors on adipogenesis and hypoxia inducible factor 1 α levels under normoxic conditions. *J. Cell. Biochem.* **101**, 1545–1557 (2007).
25. Kudo, T. et al. Context-dependent regulation of lipid accumulation in adipocytes by a HIF1 α -PPAR γ feedback network. *Cell. Syst.* **14**, 1074–1086e7 (2023).
26. He, Q. et al. Regulation of HIF-1 α activity in adipose tissue by obesity-associated factors: Adipogenesis, insulin, and hypoxia. *Am. J. Physiol. Endocrinol. Metab.* **300**, (2011).
27. White, U. & Ravussin, E. Dynamics of adipose tissue turnover in human metabolic health and disease. *Diabetologia.* **62**, 17–23 (2019).
28. Spalding, K. L. et al. Dynamics of fat cell turnover in humans. *Nature* **453**, 783–787 (2008).
29. Yin, J. et al. Role of hypoxia in obesity-induced disorders of glucose and lipid metabolism in adipose tissue. *Am. J. Physiol. Endocrinol. Metab.* **296**, E333–E342 (2009).
30. Musutova, M. et al. The effect of hypoxia and metformin on fatty acid uptake, storage, and oxidation in L6 differentiated myotubes. *Front. Endocrinol. (Lausanne).* **9**, 616 (2018).
31. Felix, J. B., Cox, A. R. & Hartig, S. M. Acetyl-CoA and metabolite fluxes regulate white adipose tissue expansion. *Trends Endocrinol. Metab.* **32**, 320 (2021).
32. Holleran, A. L., Briscoe, D. A., Fiskum, G. & Kelleher, J. K. Glutamine metabolism in AS-30D hepatoma cells. Evidence for its conversion into lipids via reductive carboxylation. *Mol. Cell. Biochem.* **152**, 95–101 (1995).
33. DeBerardinis, R. J. et al. Beyond aerobic glycolysis: Transformed cells can engage in glutamine metabolism that exceeds the requirement for protein and nucleotide synthesis. *Proc. Natl. Acad. Sci. U S A.* **104**, 19345–19350 (2007).
34. Metallo, C. M. et al. Reductive glutamine metabolism by IDH1 mediates lipogenesis under hypoxia. *Nature.* **481**, 380–384 (2011).
35. Zhang, G. F. et al. Reductive TCA cycle metabolism fuels glutamine- and glucose-stimulated insulin secretion. *Cell. Metab.* **33**, 804–817e5 (2021).
36. Xu, H. et al. Acyl-CoA synthetase short-chain family member 2 (ACSS2) is regulated by SREBP-1 and plays a role in fatty acid synthesis in caprine mammary epithelial cells. *J. Cell. Physiol.* **233**, 1005–1016 (2018).
37. Zhao, S. et al. Dietary fructose feeds hepatic lipogenesis via microbiota-derived acetate. *Nature* **579**, 586–591 (2020).
38. Smith, S. B. & Crouse, J. D. Relative contributions of acetate, lactate and glucose to lipogenesis in bovine intramuscular and subcutaneous adipose tissue. *J. Nutr.* **114**, 792–800 (1984).
39. Gao, X. et al. Acetate functions as an epigenetic metabolite to promote lipid synthesis under hypoxia. *Nature Communications* **7**, 1–14 (2016).

40. Kamphorst, J. J., Chung, M. K., Fan, J. & Rabinowitz, J. D. Quantitative analysis of acetyl-CoA production in hypoxic cancer cells reveals substantial contribution from acetate. *Cancer & Metabolism* **2**, 1–8 (2014).
41. Weiszenstein, M. et al. The Effect of Pericellular Oxygen levels on Proteomic Profile and Lipogenesis in 3T3-L1 differentiated Preadipocytes cultured on gas-permeable cultureware. *PLoS One*. **11**, e0152382 (2016).
42. Pavlacký, J. & Polak, J. Technical feasibility and physiological relevance of hypoxic cell culture models. *Front. Endocrinol. (Lausanne)* **11**, (2020).
43. Vacek, L. et al. Hypoxia induces saturated fatty acids Accumulation and reduces unsaturated fatty acids independently of reverse tricarboxylic acid cycle in L6 myotubes. *Front. Endocrinol. (Lausanne)*. **13**, 663625 (2022).
44. Ong, C. W., O'Driscoll, D. M., Truby, H., Naughton, M. T. & Hamilton, G. S. The reciprocal interaction between obesity and obstructive sleep apnoea. *Sleep. Med. Rev.* **17**, 123–131 (2013).
45. Reinke, C., Bevans-Fonti, S., Drager, L. F., Shin, M. K. & Polotsky, V. Y. Effects of different acute hypoxic regimens on tissue oxygen profiles and metabolic outcomes. *J. Appl. Physiol.* **111**, 881–890 (2011).
46. Lu, H., Gao, Z., Zhao, Z., Weng, J. & Ye, J. Transient hypoxia reprograms differentiating adipocytes for enhanced insulin sensitivity and triglyceride accumulation. *International Journal of Obesity* **2016** *40*:1 **40**, 121–128 (2015).
47. Shevchenko, A. & Simons, K. Lipidomics: Coming to grips with lipid diversity. *Nat. Rev. Mol. Cell Biol.* **11**(8), 593–598 (2010).
48. Smolková, K. & Ježek, P. The role of mitochondrial NADPH-dependent isocitrate dehydrogenase in cancer cells. *Int. J. Cell. Biol.* <https://doi.org/10.1155/2012/273947> (2012).
49. Handy, D. E. & Loscalzo, J. Responses to reductive stress in the cardiovascular system. *Free Radic Biol. Med.* **109**, 114–124 (2017).
50. Kampjut, D. & Sazanov, L. A. Structure and mechanism of mitochondrial proton-translocating transhydrogenase. *Nature*. **573**, 291–295 (2019).
51. Zhang, Z. et al. Serine catabolism generates liver NADPH and supports hepatic lipogenesis. *Nat. Metab.* **3**, 1608 (2021).
52. Ducluzeau, P. H. et al. Dynamic regulation of mitochondrial network and oxidative functions during 3T3-L1 fat cell differentiation. *J. Physiol. Biochem.* **67**, 285–296 (2011).
53. Metallo, C. M. et al. Reductive glutamine metabolism by IDH1 mediates lipogenesis under hypoxia. *Nature* **481**, 380–384 (2011).
54. Zhao, S. et al. ATP-Citrate lyase controls a glucose-to-acetate metabolic switch. *Cell. Rep.* **17**, 1037–1052 (2016).
55. Schug, Z. T. et al. Acetyl-CoA synthetase 2 promotes acetate utilization and maintains Cancer Cell Growth under metabolic stress. *Cancer Cell*. **27**, 57–71 (2015).
56. Wheatley, V. R., Hodgins, L. T., Coon, W. M. & Cutaneous Lipogenesis, I. Evaluation of Model systems and the utilization of acetate, citrate and glucose as compared with other tissues. *J. Invest. Dermatology*. **54**, 288–297 (1970).
57. Murphy, A. M. et al. Intermittent hypoxia in obstructive sleep apnoea mediates insulin resistance through adipose tissue inflammation. *Eur. Respir. J.* **49**, 1601731 (2017).
58. Tang, Y., Wang, J., Cai, W. & Xu, J. RAGE/NF-κB pathway mediates hypoxia-induced insulin resistance in 3T3-L1 adipocytes. *Biochem. Biophys. Res. Commun.* **521**, 77–83 (2020).
59. Magalang, U. J. et al. Intermittent hypoxia suppresses adiponectin secretion by adipocytes. *Experimental Clin. Endocrinol. Diabetes*. **117**, 129–134 (2009).
60. Dunlop, M. & Court, J. M. Lipogenesis in developing human adipose tissue. *Early Hum. Dev.* **2**, 123–130 (1978).
61. Zebisch, K., Voigt, V., Wabitsch, M. & Brandsch, M. Protocol for effective differentiation of 3T3-L1 cells to adipocytes. *Anal. Biochem.* **425**, 88–90 (2012).
62. Si, Y., Yoon, J. & Lee, K. Flux profile and modularity analysis of time-dependent metabolic changes of de novo adipocyte formation. *Am. J. Physiol. Endocrinol. Metab.* **292**, 1637–1646 (2007).
63. Dvořák, A., Zelenka, J., Smolková, K., Vitek, L. & Ježek, P. Background levels of neomorphic 2-hydroxyglutarate facilitate proliferation of primary fibroblasts. *Physiol. Res.* **66**, 293–304 (2017).
64. Yoshimoto, M. et al. Characterization of acetate metabolism in tumor cells in relation to cell proliferation: Acetate metabolism in tumor cells. *Nucl. Med. Biol.* **28**, 117–122 (2001).
65. Yoshii, Y. et al. Tumor uptake of radiolabeled acetate reflects the expression of cytosolic acetyl-CoA synthetase: Implications for the mechanism of acetate PET. *Nucl. Med. Biol.* **36**, 771–777 (2009).
66. Vankoningsloo, S. et al. Mitochondrial dysfunction induces triglyceride accumulation in 3T3-L1 cells: Role of fatty acid β-oxidation and glucose. *J. Lipid Res.* **46**, 1133–1149 (2005).
67. Blish, E. G. & Dyer, W. J. A rapid method of total lipid extraction and purification. *Can. J. Biochem. Physiol.* **37**, 911–917 (1959).
68. Bradford, M. M. A rapid and sensitive method for the quantitation of microgram quantities of protein utilizing the principle of protein-dye binding. *Anal. Biochem.* **72**, 248–254 (1976).
69. Lu, Y. et al. Inhibition of ACSS2 attenuates alcoholic liver steatosis via epigenetically regulating de novo lipogenesis. *Liver Int.* **43**, 1729–1740 (2023).

Acknowledgements

The authors would like to thank Dr Vladimir Krylov for providing the radioisotope laboratory and Sarka Fleischerova for technical assistance. The present study was supported by the Ministry of Health of the Czech Republic project AZV (NU21-01-00259), by the Grant Agency of Charles University (project GAUK 294822), by the Charles University research program Cooperatio Metabolic Diseases and by the Ministry of Health of the Czech Republic project MH CZ-DRO-VFN64165.

Author contributions

L.R. performed qPCR, lipid assays and experiments exploring the ¹³C-glutamine, ¹⁴C-glucose and ¹⁴C-acetate incorporation to lipids, analyzed and graphed the data, and drafted the manuscript. K.P., A.D. performed and interpreted the results of GC-MS analysis. L.V. supervised and interpreted the results of GC-MS analysis. J.V. performed and interpreted the results of radioactively labelled glucose and acetate studies. T.W. performed and analyzed the lipid assay. J.P. designed and conducted the whole study, analyzed the data and drafted the manuscript. All authors have participated in the manuscript preparation and approved the final form.

Declarations

Competing interests

The authors declare no competing interests.

Additional information

Correspondence and requests for materials should be addressed to J.P.

Reprints and permissions information is available at www.nature.com/reprints.

Publisher's note Springer Nature remains neutral with regard to jurisdictional claims in published maps and institutional affiliations.

Open Access This article is licensed under a Creative Commons Attribution-NonCommercial-NoDerivatives 4.0 International License, which permits any non-commercial use, sharing, distribution and reproduction in any medium or format, as long as you give appropriate credit to the original author(s) and the source, provide a link to the Creative Commons licence, and indicate if you modified the licensed material. You do not have permission under this licence to share adapted material derived from this article or parts of it. The images or other third party material in this article are included in the article's Creative Commons licence, unless indicated otherwise in a credit line to the material. If material is not included in the article's Creative Commons licence and your intended use is not permitted by statutory regulation or exceeds the permitted use, you will need to obtain permission directly from the copyright holder. To view a copy of this licence, visit <http://creativecommons.org/licenses/by-nc-nd/4.0/>.

© The Author(s) 2024